IEEE Photonics Journal
An IEEE Photonics Society Publication

Open Access

An Optically Transparent Ultrabroadband Microwave Absorber

Volume 9, Number 6, December 2017

Senfeng Lai
Yanghui Wu
Xiaobo Zhu
Wenhua Gu
Wen Wu

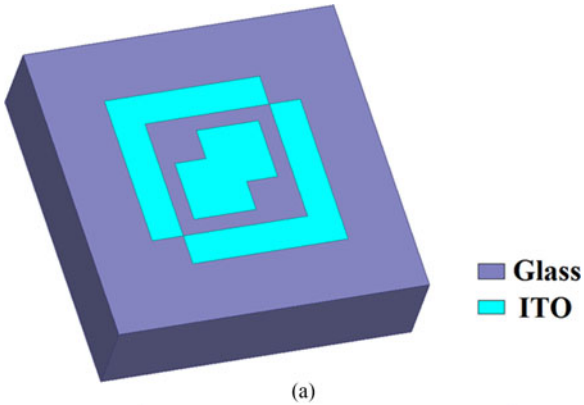

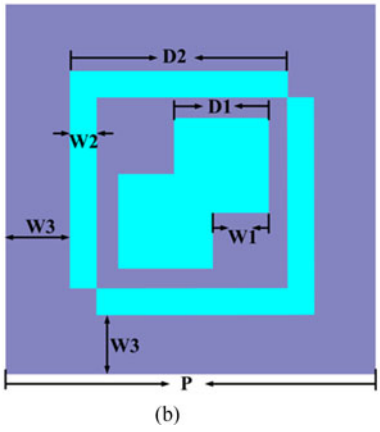

DOI: 10.1109/JPHOT.2017.2763640
1943-0655 © 2017 IEEE

An Optically Transparent Ultrabroadband Microwave Absorber

Senfeng Lai, Yanghui Wu, Xiaobo Zhu, Wenhua Gu, and Wen Wu

School of Electronic and Optical Engineering, Nanjing University of Science and Technology, Nanjing 210094, China

DOI:10.1109/JPHOT.2017.2763640

Manuscript received September 11, 2017; revised October 9, 2017; accepted October 12, 2017. Date of publication October 20, 2017; date of current version October 31, 2017. This work was supported by the National Natural Science Foundation of China under Grant 61627802, the fundamental research funds for the central universities under Grant 30917012202, and the Innovation Talent Program of Jiangsu Province. Corresponding author: W. Gu (e-mail: guwenhua@njust.edu.cn).

Abstract: An optically transparent ultrabroadband microwave absorber was proposed and experimentally verified, which achieved 23.4-GHz deep absorption bandwidth (absorption $>$0.8 from 15.6 to 39.0 GHz). What is more, the whole absorber is transparent in the visible light range (transmittance $>$0.8 from 400 to 1100 nm). The absorber thickness was 1.1 mm only, about 1/10 of the center wavelength (9.23 mm, or 32.5 GHz), and can be further reduced. Further analysis showed that the absorber was insensitive to the polarization angle and dropped only little for incident angles smaller than 30°. In general, this absorber can achieve ultrabroadband low reflection in both visible-light and microwave frequencies, providing a new solution for the design of stealth systems.

Index Terms: Transparent, ultra-broadband, microwave absorber.

1. Introduction

The optically transparent microwave system is a thriving research topic. Examples including transparent RFID system [1], graphene-based transparent THz waveband absorber [2], and others [3]–[12]. Among them, the ultra-broadband microwave absorber is of special interest, because it has important applications in antenna design [3], filter structure [4], electromagnetic shielding [5], [6] and electromagnetic compatibility [7], [8]. As a mature transparent conducting oxide, indium tin oxide (ITO) has been used in the design of transparent microwave absorbers, usually in narrow bands though [9]–[11]. The main ideas include to use ITO as the ground plane [12] to replace metal conductors, and to simply pack multiple ITO films to increase the microwave absorption ratio [9]. Hanazawa M. et al. used ITO layers with different sheet resistance on top of PET, to realize X waveband absorption (7-11.2 GHz) [13]. Similarly, Takizawa K et al. adjusted the sheet resistance and spacing of top and bottom ITO layers to achieve absorption at 60 GHz [14].

An optically transparent ultra-broadband metamaterial absorber based on ITO glass is proposed in this article. The design idea is to use ITO as the transparent conducting material on top and bottom of glass medium, and to form metamaterials with designed equivalent impedance at the given frequency range through special structure design, thus realizing ultra-broadband absorption.

Also, many research work has been reported to achieve ultra-broad absorbing bandwidth [15]–[24], most not transparent though. For example, Ghosh S. et al. used multiple resonance units to

increase the numbers of absorbing peak [25]–[29], Ding F. et al. used multiple-layer metal resonance structures with different sizes to increase the absorbing bandwidth [13], [30]–[32]. However, the additional thickness or layers to achieve broad bandwidth will increase the difficulty and cost of fabrication, thus limiting the practical applications. Therefore, development of thin ultra-broadband absorber becomes important [13]. The proposed transparent absorber has a thickness of 1.1 mm, only about 1/10 of the center wavelength (9.23 mm for 32.5 GHz), which is thin enough and can still be further reduced.

In general, the proposed ITO-based microwave absorber has the merits of optically transparent, ultra-broadband microwave absorption, thin structure, and easy and cost-effective fabrication.

2. Design and Simulation

The metamaterial absorber has a Metal-Dielectric-Metal sandwich structure, with ITO as the top resonance structure array layer, glass as the medium layer, and another ITO as the bottom ground layer which covers the whole surface. When the EM wave incidents into the structure surface, the top resonance structure will form surface current causing electric resonance, and the top and bottom layer together will form anti-parallel current thus causing magnetic resonance. By reasonably designing the geometric shape and size of the top resonance structure array, the electric resonance and the magnetic resonance can overlap in the same bandwidth, thus both the electric field energy and the magnetic field energy can be absorbed in this band, realizing perfect absorption (absorption ratio close to 1).

The absorption ratio can be calculated by Eq. (1), where f is the incident frequency, $A(f)$ is the ratio of absorption power, $R(f)$ is the ratio of reflection power, $T(f)$ is the ratio of transmission power, and $S_{11}(f)$ and $S_{21}(f)$ are the corresponding S parameters.

$$A(f) = 1 - R(f) - T(f) = 1 - \left|S_{11}(f)\right|^2 - \left|S_{21}(f)\right|^2 \tag{1}$$

For transmittance $T(f)$, because the bottom ground ITO layer has very high conductivity in the microwave range (close to PEC), $T(f)$ is close to 0, or S_{21} is close to 0. So Eq. (1) can be rewritten as:

$$A(f) = 1 - R(f) = 1 - \left|S_{11}(f)\right|^2 \tag{2}$$

The $R(f)$ can be calculated by Eq. (3):

$$R(f) = \frac{Z(f) - Z_0}{Z(f) + Z_0} \tag{3}$$

Here $Z(f)$ is the impedance of the absorbing structure, which can be calculated by Eq. (4):

$$Z(f) = \sqrt{\frac{\mu_r(f) \bullet \mu_0}{\varepsilon_r(f) \bullet \varepsilon_0}} \tag{4}$$

And Z_0 is the impedance in the free space, or

$$Z_0 = \sqrt{\frac{\mu_0}{\varepsilon_0}} \approx 377\ \Omega \tag{5}$$

where μ_0 is the permeability in vacuum, and ε_0 is the permittivity in vacuum. Thus we can see that, the design objective is to adjust the structure parameters of the top ITO layer to optimize the equivalent μ_r and ε_r of the metamaterial, so that the absorber impedance $Z(f)$ equals to the free space impedance Z_0, thus achieving minimum $R(f)$ (close to 0).

The optimized resonance structure array unit is illustrated in Fig. 1. The unit has two overlapped solid squares at the center, surrounded by a square split-ring.

ANSYS HFSS was used for the absorption spectrum simulation. To simulate the array structure of the metamaterial, Foloquet port and master-slave boundary condition were set in the software,

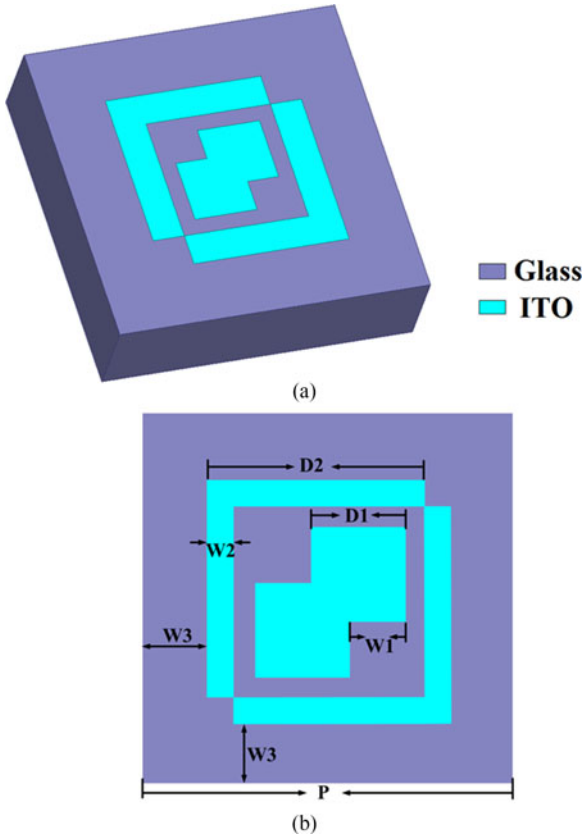

Fig. 1. Schematic of a unit cell of the proposed absorber. (a) The 3D schematic and (b) the top view.

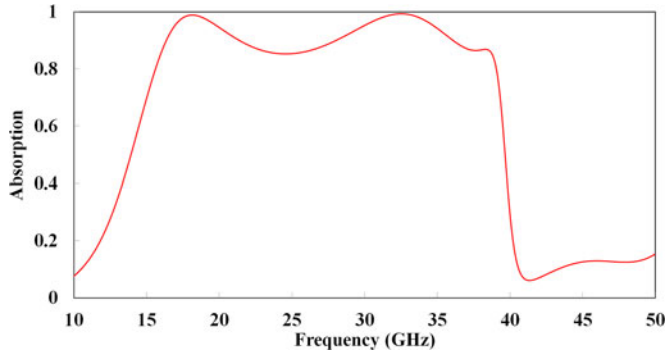

Fig. 2. Simulated absorption spectrum of the ITO absorber for the normal incidence EM wave.

with the unit structure periodically repeated in the X and Y directions. The optimized structure parameters were: $D1 = 800\,\mu$m, $D2 = 2000\,\mu$m, $W1 = 400\,\mu$m, $W2 = 400\,\mu$m, $W3 = 800\,\mu$m, and $P = 4000\,\mu$m. The glass slide thickness was 1.1 mm, and the relative permittivity was 5.5. The ITO coating thickness was 185 nm, with a sheet resistance of 8 $\Omega/square$ and inductance 0. The simulation result is shown in Fig. 2.

It can be seen from Fig. 2 that the full-width-half-maximum (FWHM) bandwidth reaches 25.7 GHz (from 13.9 GHz to 39.6 GHz). Or, if we use absorption ratio $>$0.8 as the criterion, the high-absorption band reaches 23.4 GHz, (from 15.6GHz to 39GHz). Both are ultra-broad. There are two absorption peaks, one at 18.1 GHz (absorption ratio 0.990) , and one at 32.5 GHz (absorption ratio 0.992).

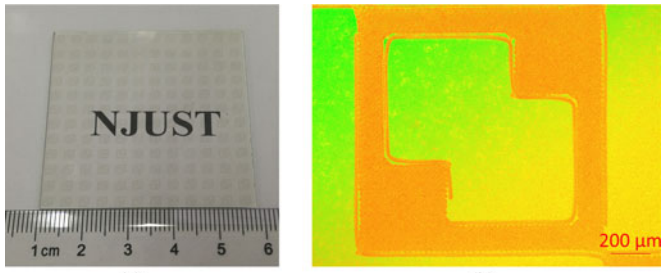

Fig. 3. Fabricated prototype of the proposed ITO absorber. (a) Overall size image, with a white paper printed with "NJUST" put underneath to illustrate the sample transparency. (b) Microscope picture of a unit cell of the ITO absorber.

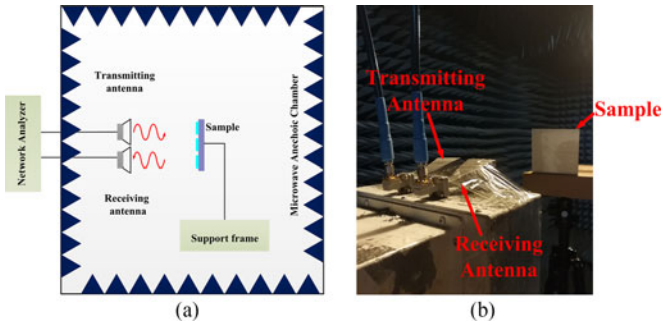

Fig. 4. (a) Schematic diagram of test system. (b) Actual test system.

3. Experiments

The ITO was sputtered onto the 1.1 mm glass slide substrate, followed with wet-etching to obtain the metamaterial structure. The whole fabrication process was very straightforward and used mature industrial techniques, with high potential of mass production. The fabricated sample is shown in Fig. 3.

The test system is illustrated and pictured in Fig. 4(a) and (b).

The experiment was performed in a microwave anechoic chamber, and the S_{11} parameter was measured by a vector network analyzer (Rohde&Schwarz ZVA 67). The sample size was 9.6 mm $*$ 9.6 mm. Three sets of standard horn antennas were used in the measurement to cover different wavebands: 15.0 GHz-22.0 GHz, 18.0 GHz-26.5 GHz, and 26.5 GHz-40.0 GHz. A flat copper board was used as the PEC reference reflection plane for calibration of the system [33], and the measured S_{11} was used as the reference signal of complete reflection. Then the sample shown in Fig. 3 was placed at the exactly same location, and the difference between the measured reflection signal from the sample and from the reference copper board was used as the sample reflection S_{11} signal. The absorption can be calculated from the S_{11} values using Eq. (2). The measured absorption spectrum is shown in Fig. 5, matching pretty well with the simulation results. Possible error origins include the noise during testing as well as the fabrication error.

The optical transmission spectrum of the sample was also measured from 250 nm to 10000 nm (10 μm), using an ultraviolet-visible-infrared spectrometer (Evolution 220) together with a home-made infrared spectrometer, to cover a very broad waveband from ultraviolet through visible light all the way to mid-infrared, as shown in Fig. 6. The inset shows the transmission spectrum from 250 nm to 1050 nm, where the whole transmission curve was above 0.8. The ITO film is well-known for its transparency in the visible light region, and it has strong reflection in the middle and far infrared region, mainly due to excitation of surface plasmonic wave [34]–[37].

From Fig. 6 we can see that in the ultraviolet waveband from 250 nm to 300 nm, the transmittance was almost 0, and the transmittance increased quickly with the wavelength increasing from 300 nm

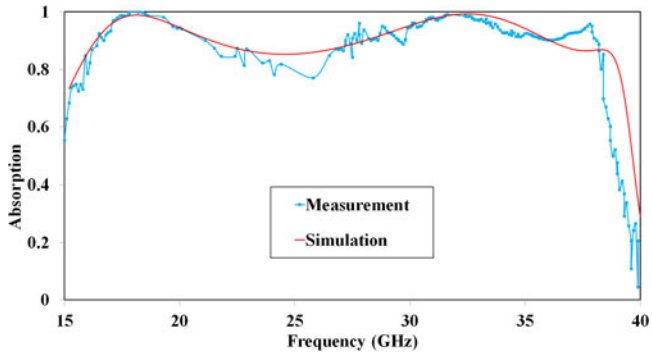

Fig. 5. Comparison of the simulated and tested absorption spectra of the ITO absorber.

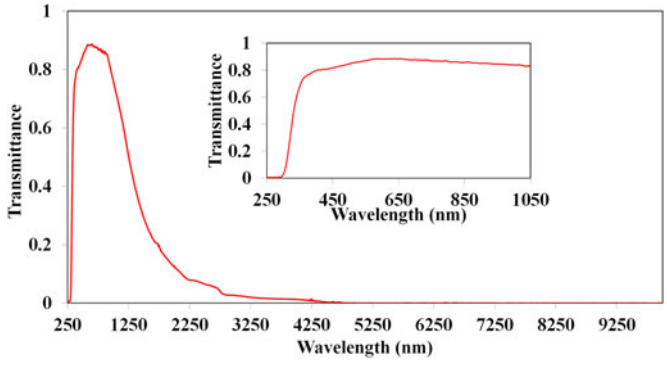

Fig. 6. Transmission spectrum at 250–10 000 nm range. The inset shows the details of part the transmission spectrum from 250 to 1050 nm.

to 400 nm. The transmittance in the whole visible light range was above 0.84, so the sample was very transparent in the visible light range. Yet in the long wavelength range, from 2.5 μm to 10 μm, the transmittance was almost 0. Therefore, in the measured light waveband, this sample worked as a band-pass filter, with the transmission window in the visible light waveband. This property, together with the ultra-broadband microwave absorption characteristic, makes the sample a perfect stealth system.

It may be worthy to mention that many transparent absorber designs still rely on metal wires as electric current carriers, and are transparent only in the area without metal coverage. Thanks to the transparency of ITO, the proposed absorber is transparent in all the area.

4. Discussion and Analysis

4.1 Space Distribution of Electric Currents and Fields

To better understand the ultra-broadband absorption characteristic of the metamaterial absorber, detailed simulation was performed to analyze the space distribution of the electric currents and fields. At the two peak absorption frequencies, i. e., 18.1 GHz and 32.5 GHz, the distribution of the surface electric currents is shown in Fig. 7.

From Fig. 8 we can see that strong electric fields appeared at the edge of the split ring and the gap between the split ring and the overlapped squares, and the electric field at the edge of the overlapped squares was also very strong. Strong electric field means existence of strong electric field resonance. From the electric current distribution at the top and bottom surfaces shown in Fig. 7, it can be seen that the high electric current values appeared at the two arms of the split rings. At the same time, at the absorption peak, the electric current at the top and bottom surfaces were anti-parallel, so that the electric current could form magnetic dipole, which then generate strong

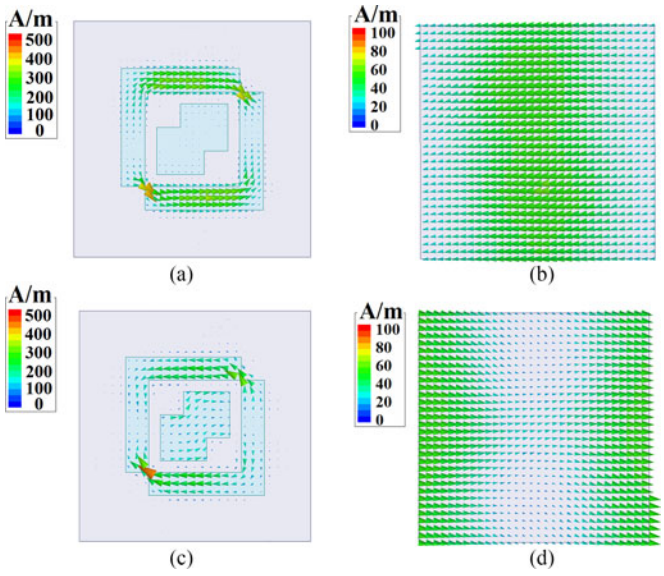

Fig. 7. Space distribution of the surface current on (a) top and (b) bottom surface at 18.1 GHz, and that on (c) top and (d) bottom surface at 32.5 GHz.

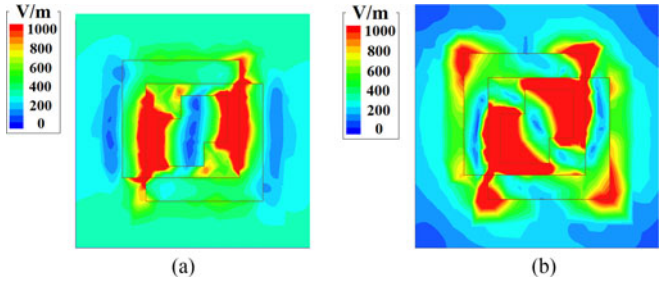

Fig. 8. Space distribution of the electric field at (a) 18.1 GHz and (b) 32.5 GHz on the top surface.

magnetic resonance at the resonance frequencies. Therefore, the resonance array structure at the top ITO layer can adjust the equivalent permittivity or the electric response, and the combination of the top and bottom ITO layers can adjust the equivalent permeability or the magnetic response. According to Eqs. (2)–(4), when the equivalent permittivity and permeability were adjusted to proper values, the structure could have an equivalent impedance matching the free space impedance, thus the absorption would be very close to 1. This is the objective of the structure optimization during simulation.

4.2 Equivalent Circuit Analysis

The equivalent circuit model of the designed absorber is illustrated in Fig. 9.

The equivalent circuit composes three parts: R_0 represent the free space characteristic impedance (resistance only), a parallel connection of three *RLC* serial circuits represents the top ITO layer equivalent impedance, and C_d and L_d represent the capacitor and inductor of the transmission line formed by the glass medium and the bottom ITO layer. For the top ITO layer, the *R, L*, and *C* represent the equivalent resistor, inductor, and capacitor, respectively, and the three circuits represents the equivalent circuits for the two arms of the split ring as well as the overlapped squares.

Quantitative simulation was performed by Advanced Design System (ADS), and thus-obtained absorption curve was plotted and compared to the HFSS simulation result in Fig. 10, where the

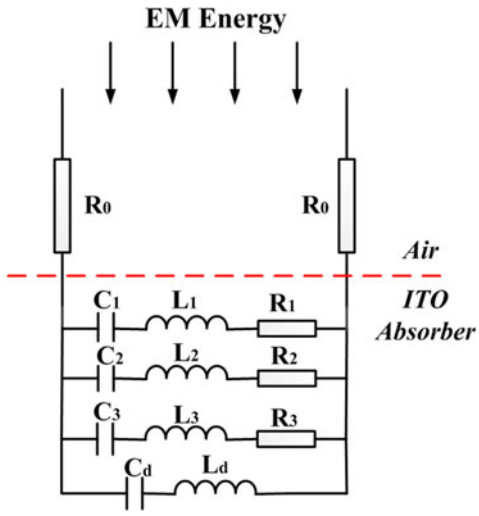

Fig. 9. The equivalent circuit of the proposed ITO absorber.

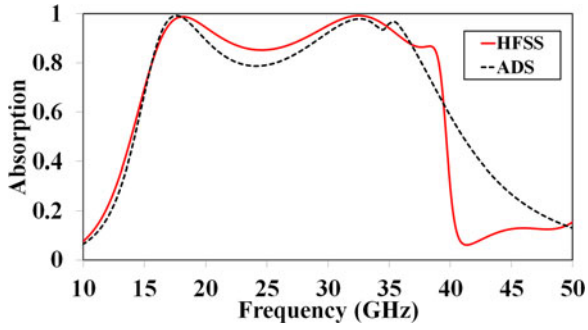

Fig. 10. Comparison of the absorption spectrum calculated by HFSS and ADS.

TABLE 1
Calculated Parameters of the Equivalent Circuit

R_1	R_2	R_3	C_1	C_2	C_3
0.05 Ohm	140 Ohm	1080.02 Ohm	40 fF	26 fF	0.15 fF
L_1	**L_2**	**L_3**		**Ld**	**Cd**
0.9 fH	1.65×10^6 fH	139.45×10^6 fH		11×10^5 fH	24.96×10^3 fF

red solid line is the curve obtained from HFSS, and the black dotted line is the curve obtained from ADS. They match reasonably well.

Calculated parameters of the equivalent circuit are shown in the Table 1.

The impedance of the absorber normalized to Z_0 at different frequencies can be calculated by Eq. (6) [38], [39], and is plotted in Fig. 11. At the two absorption peaks (labelled in Fig. 11), the real part of the normalized impedance was close to 1, and the imaginary part close to 0, which means the normalized impedance at these two frequency points could match very well with the free space

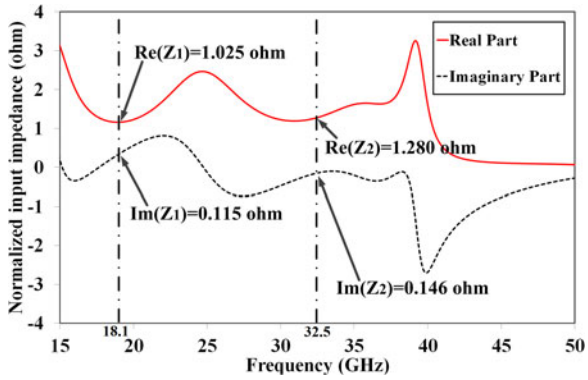

Fig. 11. Normalized input impedance of the proposed ITO absorber.

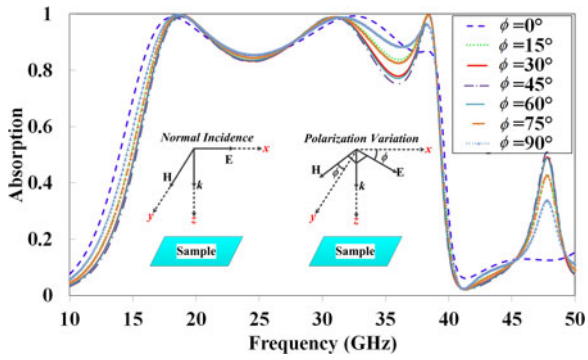

Fig. 12. Absorption spectra at different polarization angles under normal incident EM wave.

impedance, so that perfect absorption was achieved.

$$Z = \pm\sqrt{\frac{(1+S_{11})^2 - S_{21}^2}{(1-S_{11})^2 - S_{21}^2}} = \pm\frac{1+S_{11}}{1-S_{11}} \tag{6}$$

4.3 Dependence on the Polarization Angle and Incident Angle

All the above analysis was based on zero polarization angle ϕ of the incident wave. However, a perfect absorber requires insensitivity to the polarization angle. So the absorption spectrum dependence on the polarization angle was studied by simulation, as illustrated in Fig. 12. It can be clearly seen that the impact of polarization angle to the absorption was pretty small, or the designed absorber is insensitive to the polarization angle. The polarization insensitivity can be attributed the geometric axial symmetry of the top ITO layer design.

Another concern is the absorption spectrum dependence on the incident angle. Impact of different incident angle θ was also studied, and the results are shown in Fig. 13.

It can be seen from Fig. 13 that the absorption curve dropped with the incident angle, and in general TM polarization dropped faster than TE polarization. However, for $\theta \leq 30^\circ$, the absorption spectrum change was relatively small. Even at $\theta = 30^\circ$, the high absorption band (absorption $>$0.8) was still ultra-broad, i.e., from 15 GHz to 40 GHz for TE polarization, and from 15 GHz to 35 GHz for TM polarization. This $\theta \leq 30^\circ$ condition is true for most practical cases, where the incident wave is usually far away from the object so that the incident angle is very close to 0. So in practice the absorption spectrum dependence on the incident angle can usually be neglected as well.

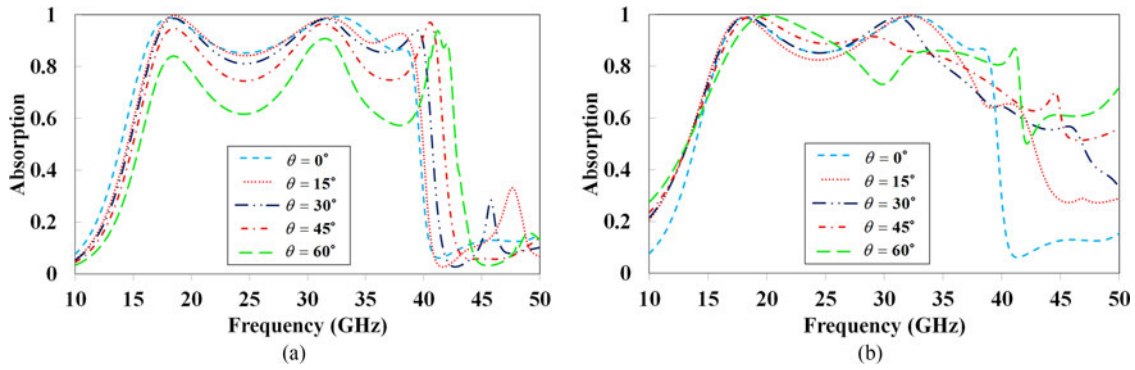

Fig. 13. Absorption spectrum at different incident angle for (a) TE polarization and (b) TM polarization.

5. Conclusion

An optically transparent ultra-broadband microwave absorber based on ITO glass was designed and tested. The absorption performance was verified by simulation and experiments, with absorption ratio $>$0.8 between 15.6 GHz and 39.1 GHz. At the same time, the whole absorber was transparent in the visible light range, with very low transmittance in the ultraviolet and infrared wavebands. The equivalent circuit of the absorber was modeled and calculated, revealing that impedance matching with the free space was key to the perfect absorption characteristics. The absorber was insensitive to the polarization angle. For incident angle less than 30°, the change of the absorption spectrum can be neglected. All these results prove that this new design of absorber can be a useful tool for advanced stealth systems and other applications.

Acknowledgment

The authors would like to thank Prof. Shilong Pan's group from Nanjing University of Aeronautics and Astronautics for help in microwave band measurement and Prof. Chuanxiang Sheng's group from Nanjing University of Science and Technology for help in visible and infrared band measurement.

References

[1] Y. Yao, J. Yu, and X. Chen, "Study on the optically transparent near-field and far-field RFID reader antenna," *Int. J. Antennas Propag.*, vol. 2014, pp. 1–5, 2014.
[2] B. Wu *et al.*, "Experimental demonstration of a transparent graphene millimetre wave absorber with 28% fractional bandwidth at 140 GHz," *Sci. Rep.*, vol. 4, 2014, Art. no. 4130.
[3] C. Singh, K. R. Jha, V. Singh, and G. Singh, "Cross-polarization reduction of microstrip antenna using microwave absorbers," *Int. J. Rf Microw. Comput.-Aided Eng.*, vol. 27, 2017, Art. no. e21088.
[4] Fang W and Xu S. "New Electromagnetic Absorbers Composed of Left-handed and Right-handed Materials," *Int. J. Infrared Millimeter Waves*, vol. 29, pp. 799–807, 2008.
[5] M. N. Iqbal, M. F. B. A. Malek, S. H. Ronald, M. S. B. Mezan, K. M. Juni, and R. Chat, "A study of the EMC performance of a graded-impedance, microwave, rice-husk absorber," *Prog. Electromagn. Res.*, vol. 131, pp. 19–44, 2012.
[6] T. M. Kollatou, S. D. Assimonis, and C. S. Antonopoulos, "A family of ultra-thin, octagonal shaped microwave absorbers for EMC applications," *Mater. Sci. Forum*, vol. 792, pp. 165–170, 2014.
[7] T. M. Kollatou, A. I. Dimitriadis, N. V. Kantartzis, M. Hinaje, and C. S. Antonopoulos, "A class of multi-band, polarization-insensitive, microwave metamaterial absorbers in EMC analysis," in *Proc. Int. Symp. Electromagn. Compat.*, 2012, pp. 1–4.
[8] P. Saville, *Review of Radar Absorbing Materials*. Ottawa, ON, Canada: Defence Res. Develop. Canada, 2005.
[9] X. Wang, B. Zhang, W. Wang, J. Wang, and J. Duan, "Design and characterization of an ultrabroadband metamaterial microwave absorber," *IEEE Photon. J.*, vol. 9, no. 3, Jun. 2017, Art. no. 4600213.
[10] D. Lee, H. K. Sung, and S. Lim, "Flexible subterahertz metamaterial absorber fabrication using inkjet printing technology," *Appl. Phys. B*, vol. 122, pp. 1–8, 2016.
[11] N. I. Landy, C. M. Bingham, T. Tyler, N. Jokerst, D. R. Smith, and W. J. Padilla, "Design, theory, and measurement of a polarization insensitive absorber for terahertz imaging," *Phys. Rev. B Condensed Matter Mater. Phys.*, vol. 79, 2008, Art. no. 125104.

[12] B. Wang, T. Koschny, and C. M. Soukoulis, "Wide-angle and polarization-independent chiral metamaterial absorber," *Phys. Rev. B*, vol. 80, 2010, Art. no. 033108.
[13] G. Dayal and S. A. Ramakrishna, "Broadband infrared metamaterial absorber with visible transparency using ITO as ground plane," *Opt. Exp.*, vol. 22, pp. 15104–15110, 2014.
[14] K. Takizawa and O. Hashimoto, "Transparent wave absorber using resistive thin film at V-band frequency," *IEEE Trans. Microw. Theory Techn.*, vol. 47, no. 7, pp. 1137–1141, Jul. 1999.
[15] Y. Cheng, H. Yang, Z. Cheng, and B. Xiao, "A planar polarization-insensitive metamaterial absorber," *Photon. Nanostruct.—Fundam. Appl.*, vol. 9, pp. 8–14, 2011.
[16] H. Tao, N. I. Landy, C. M. Bingham, X. Zhang, R. D. Averitt, and W. J. Padilla, "A metamaterial absorber for the terahertz regime: Design, fabrication and characterization," *Opt. Exp.*, vol. 16, pp. 7181–7188, 2008.
[17] D. Y. Shchegolkov, A. K. Azad, J. F. O'Hara, and E. I. Simakov, "Perfect subwavelength fishnetlike metamaterial-based film terahertz absorbers," *Phys. Rev. B Condensed Matter*, vol. 82, 2010, Art. no. 205117.
[18] Z. H. Jiang, S. Yun, F. Toor, D. H. Werner, and T. S. Mayer, "Conformal dual-band near-perfectly absorbing mid-infrared metamaterial coating," *ACS Nano*, vol. 5, pp. 4641–4647, 2011.
[19] X. Liu, T. Starr, A. F. Starr, and W. J. Padilla, "Infrared spatial and frequency selective metamaterial with near-unity absorbance," *Phys. Rev. Lett.*, vol. 104, 2010, Art. no. 207403.
[20] P. Ding, E. Liang, G. Cai, W. Hu, C. Fan, and Q. Xue, "Dual-band perfect absorption and field enhancement by interaction between localized and propagating surface plasmons in optical metamaterials," *J. Opt.*, vol. 13, 2011, Art. no. 075005.
[21] K. Aydin, V. E. Ferry, R. M. Briggs, and H. A. Atwater, "Broadband polarization-independent resonant light absorption using ultrathin plasmonic super absorbers," *Nature Commun.*, vol. 2, 2011, Art. no. 517.
[22] J. W. Park *et al.*, "Multi-band metamaterial absorber based on the arrangement of donut-type resonators," *Opt. Exp.*, vol. 21, pp. 9691–9702, 2013.
[23] L. Li, Y. Yang, and C. Liang, "A wide-angle polarization-insensitive ultra-thin metamaterial absorber with three resonant modes," *J. Appl. Phys.*, vol. 110, 2011, Art. no. 063702.
[24] D. T. Viet *et al.*, "Perfect absorber metamaterials: Peak, multi-peak and broadband absorption," *Opt. Commun.*, vol. 322, pp. 209–213, 2014.
[25] J. Lee and S. Lim, "Bandwidth-enhanced and polarisation-insensitive metamaterial absorber using double resonance," *Electron. Lett.*, vol. 47, pp. 8–9, 2011.
[26] S. Ghosh, S. Bhattacharyya, and K. V. Srivastava, "Design of a bandwidth-enhanced ultra thin metamaterial absorber," in *Proc. Prog. Electromagn. Res. Symp.*, 2013, pp. 1091–1101.
[27] S. Bhattacharyya, S. Ghosh, D. Chaurasiya, and K. V. Srivastava, "Bandwidth-enhanced dual-band dual-layer polarization-independent ultra-thin metamaterial absorber," *Appl. Phys. A*, vol. 118, pp. 207–215, 2014.
[28] H. Xiong, J. S. Hong, C. M. Luo, and L. L. Zhong, "An ultrathin and broadband metamaterial absorber using multi-layer structures," *J. Appl. Phys.*, vol. 114, 2013, Art. no. 064109.
[29] J. Grant, Y. Ma, S. Saha, A. Khalid, and D. R. Cumming, "Polarization insensitive, broadband terahertz metamaterial absorber," *Opt. Lett.*, vol. 36, pp. 3476–3478, 2011.
[30] F. Ding, Y. Cui, X. Ge, Y. Jin, and S. He, "Ultra-broadband microwave metamaterial absorber," *Appl. Phys. Lett.*, vol. 100, 2011, Art. no. 103506.
[31] H. Yang, X. Y. Cao, J. Gao, W. Li, Z. Yuan, and K. Shang, "Low RCS metamaterial absorber and extending bandwidth based on electromagnetic resonances," *Prog. Electromagn. Res. M*, vol. 33, pp. 31–44, 2013.
[32] Y. Okano, S. Ogino, and K. Ishikawa, "Development of optically transparent ultrathin microwave absorber for ultrahigh-frequency RF identification system," *IEEE Trans. Microw. Theory Techn.*, vol. 60, no. 8, pp. 2456–2464, Aug. 2012.
[33] D. Sood and C. C. Tripathi, "Broadband ultrathin low-profile metamaterial microwave absorber," *Appl. Phys. A*, vol. 122, pp. 1–7, 2016.
[34] C. T. Lee, Q. X. Yu, B. T. Tang, and H. Y. Lee, "Effects of plasma treatment on the electrical and optical properties of indium tin oxide films fabricated by r.f. reactive sputtering," *Thin Solid Films*, vol. 386, pp. 105–110, 2001.
[35] C. H. Yang, S. C. Lee, T. C. Lin, and S. C. Chen, "Electrical and optical properties of indium tin oxide films prepared on plastic substrates by radio frequency magnetron sputtering," *Thin Solid Films*, vol. 516, pp. 1984–1991, 2008.
[36] I. Hamberg and C. G. Granqvist, "Transparent and infrared-reflecting indium-tin-oxide films: Quantitative modeling of the optical properties," *Appl. Opt.*, vol. 24, pp. 1815–1819, 1985.
[37] A. Tamanai, T. D. Dao, M. Sendner, T. Nagao, and A. Pucci, "Mid-infrared optical and electrical properties of indium tin oxide films," *Phys. Status Solidi*, vol. 214, 2016, Art. no. 1600467.
[38] S. Bhattacharyya, S. Ghosh, and K. V. Srivastava, "Triple band polarization-independent metamaterial absorber with bandwidth enhancement at X-band," *J. Appl. Phys.*, vol. 114, 2013, Art. no. 094514.
[39] D. R. Smith, D. C. Vier, T. Koschny, and C. M. Soukoulis, "Electromagnetic parameter retrieval from inhomogeneous metamaterials," *Phys. Rev. E Statist. Nonlinear Soft Matter Phys.*, vol. 71, 2005, Art. no. 036617.